Biol. Cybern. 90, 390–399 (2004)
DOI 10.1007/s00422-004-0488-0

Biological Cybernetics

Causal transfer function analysis to describe closed loop interactions between cardiovascular and cardiorespiratory variability signals

L. Faes[1], **A. Porta**[2], **R. Cucino**[1], **S. Cerutti**[3], **R. Antolini**[1], **G. Nollo**[1]

[1] Lab. Biosegnali, Dipartimento di Fisica, Università di Trento, via Sommarive 14, 38050, Povo, Trento, Italy
[2] Dipartimento di Scienze Precliniche LITA di Vialba, Università di Milano, Milano, Italy
[3] Dipartimento di Bioingegneria, Politecnico di Milano, Milano, Italy

Received: 12 December 2003 / Accepted: 28 April 2004 / Published online: 16 July 2004

Abstract. Although the concept of transfer function is intrinsically related to an input–output relationship, the traditional and widely used estimation method merges both feedback and feedforward interactions between the two analyzed signals. This limitation may endanger the reliability of transfer function analysis in biological systems characterized by closed loop interactions. In this study, a method for estimating the transfer function between closed loop interacting signals was proposed and validated in the field of cardiovascular and cardiorespiratory variability. The two analyzed signals x and y were described by a bivariate autoregressive model, and the causal transfer function from x to y was estimated after imposing causality by setting to zero the model coefficients representative of the reverse effects from y to x. The method was tested in simulations reproducing linear open and closed loop interactions, showing a better adherence of the causal transfer function to the theoretical curves with respect to the traditional approach in presence of non-negligible reverse effects. It was then applied in ten healthy young subjects to characterize the transfer functions from respiration to heart period (RR interval) and to systolic arterial pressure (SAP), and from SAP to RR interval. In the first two cases, the causal and non-causal transfer function estimates were comparable, indicating that respiration, acting as exogenous signal, sets an open loop relationship upon SAP and RR interval. On the contrary, causal and traditional transfer functions from SAP to RR were significantly different, suggesting the presence of a considerable influence on the opposite causal direction. Thus, the proposed causal approach seems to be appropriate for the estimation of parameters, like the gain and the phase lag from SAP to RR interval, which have a large clinical and physiological relevance.

Keywords: Coherence – Linear transfer function – Cardiovascular control

Correspondence to: L. Faes
(e-mail: faes@science.unitn.it,
Tel.: +39-461-882041, Fax: +39-461-881696)

1 Introduction

Transfer function analysis is a classical engineering tool developed to describe in the frequency domain the behavior of linear time-invariant systems. Starting from the knowledge of the input and output signals, it provides a black box characterization of the system response in terms of gain and phase shift at different frequencies (Bendat and Piersol 1986). In cardiovascular variability analysis, this tool is widely applied to describe the relationship between different cardiac variables in different frequency bands, thus focusing on various underlying physiological mechanisms. Particularly, the analysis of the transfer function was used to disclose the complex mechanical and autonomic effects of respiration on heart rate (Saul et al. 1989) and on arterial pressure (Saul et al. 1991), to investigate on the phase relationships between arterial pressure and heart period at the frequency of the Mayer waves (about 0.1 Hz) and at the respiratory frequency (de Boer et al. 1985; Taylor and Eckberg 1996; Wichterle et al. 2000), and to estimate baroreflex sensitivity from the spontaneous variability of systolic pressure and heart rate (Robbe et al. 1987; Pitzalis et al. 1998; Pinna et al. 2002).

The calculation of the transfer function relies on the basic assumption that the two signals taken as input and output of the investigated system interact exclusively in an open loop, that is, the input may affect the output but the reverse does not hold. This implicit assumption may be seriously violated in the field of cardiovascular and cardiorespiratory variability, where often the analyzed signals are likely to interact in a closed loop due to the complexity of the mechanisms involved in the regulation of the cardiac function. As an example, an important contribution of the feedforward arm of the regulatory loop between systolic pressure and heart period has been observed in humans in addition to the well-known feedback regulation (Legramante et al. 2001; Nollo et al. 2002). In spite of this, in the field of cardiovascular/cardiorespiratory variability transfer function analysis is traditionally performed without accounting for causality, even in presence of a non-negligible information flow in the opposite direction of that under investigation.

The present study proposes a causal approach for the evaluation of the gain and phase of the transfer function between two variability series. The approach follows the procedure proposed by Porta et al. (2002) for the calculation of the link on a specific causal direction between two closed loop interacting series. Auto- and cross-spectral power density functions relevant to the two analyzed series are calculated by means of bivariate autoregressive model identification (Kay 1988; Baselli et al. 1997), and the model coefficients representing the influences of the output over the input process are set to zero before computing the calculation of the transfer function. The method is first validated in comparison with the traditional non-causal approach on computer simulations reproducing different open- and closed-loop interactions. It is then applied to the study of the transfer functions from respiration to systolic pressure, from respiration to heart period, and from systolic pressure to heart period in healthy young subjects. The application allows us to assess, for each analyzed pair of cardiovascular and cardiorespiratory variability series, the reliability of the traditional transfer function estimation approach in comparison to the proposed causal one.

2 Theoretical considerations

2.1 Transfer function and coherence analysis

The transfer function analysis of real physiological systems is based on the simple linear model of Fig. 1 (Bendat and Piersol 1986), in which the deterministic relationship between the input and output processes x_1 and x_2 is corrupted by the noise process n. The linear time-invariant transformation H is fully characterized in the frequency domain by the complex transfer function

$$H(f) = \frac{P_{12}(f)}{P_1(f)} \quad , \tag{1}$$

where $P_1(f)$ and $P_{12}(f)$ are respectively the power spectral density of the input process and the cross-spectral density between the input and output processes evaluated at the frequency f. The modulus and the argument of the transfer function give the gain, $G(f)$, and the phase shift, $\varphi(f)$, between x_1 and x_2 as a function of frequency, respectively.

The strength of the linear coupling between the processes x_1 and x_2 is usually quantified by means of the magnitude-squared coherence

$$\gamma^2(f) = \frac{|P_{12}(f)|^2}{P_1(f)\,P_2(f)} \tag{2}$$

a real-valued function that ranges from 0, indicating absence of linear correlation at the frequency f, and 1, indicating complete correlation at that frequency. As the coherence is inversely related to the signal-to-noise ratio at the output of the linear block in Fig. 1 (Faes et al. 2002), it is blunted when the power of n is high (e.g., in presence of sources uncorrelated with the input but affecting the output of the system) or when the power of v is low (e.g., in case of reduced variability of the input signal or low system gain).

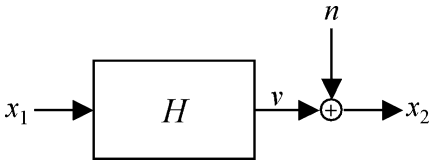

Fig. 1. Linear model for the description of the input/output relationship between two time series. The output series x_2 depends on the input series x_1, through the linear transformation H yielding the series v, and on uncorrelated sources described by the series n

In practical analysis, transfer function and coherence are derived from the available realizations of the two investigated processes by providing estimates of the auto- and cross-spectral density functions involved in (1) and (2). The two major approaches usually followed are the classical approach, based on the computation of the Fourier transform of either the windowed data or the windowed auto- and cross-covariance functions (Priestley 1981; Pinna and Maestri 2001), and the parametric approach, based on fitting a linear model to the data and evaluating the spectral functions from the model after the identification procedure (Kay 1988; Baselli et al. 1986). For both estimation approaches, transfer function and coherence are obtained by a global analysis which is unable to inform about the causal relationships occurring between the two processes under analysis.

2.2 Parametric estimation of spectral density functions

When spectral estimation is performed by the parametric approach, the interactions between x_1 and x_2 are modeled by the bivariate autoregressive (AR) process

$$\begin{aligned} x_1(t) &= \sum_{k=1}^{p} a_{11}(k)x_1(t-k) + \sum_{k=1}^{p} a_{12}(k)x_2(t-k) + w_1(t) \\ x_2(t) &= \sum_{k=0}^{p} a_{21}(k)x_1(t-k) + \sum_{k=1}^{p} a_{22}(k)x_2(t-k) + w_2(t) \end{aligned} \tag{3}$$

where w_1 and w_2 are uncorrelated zero-mean white noises with variance σ_1^2 and σ_2^2 and p is the model order. Notice that immediate (not delayed) effects are allowed from x_1 to x_2 but not from x_2 to x_1 (i.e., $a_{21}(0) \neq 0$ and $a_{12}(0) = 0$ in (3)). This restriction is necessary as loops of immediate effects prevent the identifiability of the bivariate AR process (Baselli et al. 1997).

To investigate the system properties in the frequency domain, (3) is transformed to obtain

$$\mathbf{A}(f)\,\mathbf{X}(f) = \mathbf{W}(f) \tag{4}$$

where $\mathbf{X}(f) = [X_1(f)\,X_2(f)]^{\mathrm{T}}$ and $\mathbf{W}(f) = [W_1(f)\,W_2(f)]^{\mathrm{T}}$ are respectively the Fourier transforms of the examined bivariate process and of the bivariate noise process, and the matrix $\mathbf{A}(f)$ is given by

$$\mathbf{A}(f) = \begin{pmatrix} A_{11}(f) & A_{12}(f) \\ A_{21}(f) & A_{22}(f) \end{pmatrix}$$

$$= \begin{pmatrix} 1 - \sum_{k=1}^{p} a_{11}(k)\, e^{-j2\pi fk} & - \sum_{k=1}^{p} a_{12}(k)\, e^{-j2\pi fk} \\ - \sum_{k=0}^{p} a_{21}(k)\, e^{-j2\pi fk} & 1 - \sum_{k=1}^{p} a_{22}(k)\, e^{-j2\pi fk} \end{pmatrix} \quad (5)$$

Rewriting (4) as

$$\mathbf{X}(f) = \mathbf{H}(f)\,\mathbf{W}(f) \quad (6)$$

we evidence the transfer matrix $\mathbf{H}(f)$, which results as the inverse of the coefficient matrix $\mathbf{A}(f)$.

Auto- and cross-spectral density functions are obtained as diagonal and non-diagonal elements of the power spectral density matrix

$$\mathbf{P}(f) = \mathbf{H}(f)\,\Sigma\mathbf{H}(f)^H \quad (7)$$

where Σ is the variance matrix of the bivariate noise process $[w_1 w_2]^T$, reporting the variance σ_i^2 of the white noise w_i on the diagonal and zero out of the main diagonal as a result of the uncorrelation between w_1 and w_2.

The auto spectral density functions result

$$\begin{aligned} P_1(f) &= \tfrac{1}{|\mathbf{A}(f)|^2}\left(|A_{22}(f)|^2\sigma_1^2 + |A_{12}(f)|^2\sigma_2^2\right) \\ P_2(f) &= \tfrac{1}{|\mathbf{A}(f)|^2}\left(|A_{21}(f)|^2\sigma_1^2 + |A_{11}(f)|^2\sigma_2^2\right) \end{aligned} \quad (8)$$

while the cross-spectral density function is

$$P_{12}(f) = \frac{1}{|\mathbf{A}(f)|^2} \times \left(A_{22}(f)\,A_{21}^*(f)\,\sigma_1^2 + A_{12}(f)\,A_{11}^*(f)\,\sigma_2^2\right) \quad (9)$$

2.3 Causal approach to transfer function analysis

The traditional method used to derive the transfer function and the coherence by the parametric approach is based on substituting into (1) and (2) the estimated spectral and cross-spectral density functions of (8) and (9). With this procedure, the resulting coherence is a global index of coupling merging both the causal paths described by the coefficients a_{12} and a_{21}, while the transfer function may be corrupted by the possible reverse influence of the output over the input process modeled by the block A_{12}.

To obtain a causal representation of the linear relationship from x_1 to x_2, the feedback effects are disregarded by forcing to zero the coefficients of the block A_{12} (Porta et al. 2002). In this way, the power spectral matrix becomes

$$\mathbf{P}(f) = \frac{1}{|A_{11}(f)\,A_{22}(f)|^2} \times \begin{pmatrix} |A_{22}(f)|^2\sigma_1^2 & A_{22}(f)\,A_{21}^*(f)\,\sigma_1^2 \\ A_{22}^*(f)\,A_{21}(f)\,\sigma_1^2 & |A_{21}(f)|^2\sigma_1^2 + |A_{11}(f)|^2\sigma_2^2 \end{pmatrix} . \quad (10)$$

Consequently, the causal transfer function and the causal coherence from x_1 to x_2 are defined by taking as estimates of auto- and cross-spectral density functions the diagonal and off-diagonal terms of (10), respectively.

In the following, we will indicate with $\gamma_{12}^2(f)$, $G_{12}(f)$, and $\varphi_{12}(f)$ the coherence, gain, and phase functions obtained by the traditional non-causal representation giving the spectral functions in (8) and (9), and with $\gamma_{1\to2}^2(f)$, $G_{1\to2}(f)$, and $\varphi_{1\to2}(f)$ the coherence, gain, and phase functions obtained by the causal representation giving the spectral functions in (10).

3 Methods

3.1 Simulations

The ability of the causal approach in estimating the transfer function in different conditions of linear interaction between two variability series was assessed and compared with that of the traditional non-causal approach by means of computer simulations. The adopted simulation scheme is depicted in Fig. 2a, where $[x_1\ x_2]$ is the investigated bivariate process and w_1 and w_2 are gaussian white noise processes with zero-mean and unitary variance.

In the first simulation, we set $H_{12} = 0$ to reproduce a linear open loop bivariate process. As a consequence, the input series x_1 was a realization of the noise process w_1, while the output series was obtained by the linear transformation H_{21} corrupted by the noise series w_2. The H_{21} block was realized as a finite impulse response (FIR) filter with 13 coefficients having the values reported in Fig. 2b. The modulus of the frequency response of the filter is shown in Fig. 2d (continuous line). Thanks to the particular symmetry of the filter coefficients, the phase of the frequency response is a straight line with slope of 12π radians (Oppenheim and Schafer 1975). In the second simulation, the backward influence of x_2 on x_1 was introduced to realize a closed loop bivariate process. The H_{21} block was left unchanged, while the H_{12} block was obtained as a FIR filter with nine coefficients (see Fig. 2c), having the frequency response modulus of Fig. 2d (dashed line).

For each simulation, 100 realizations of the bivariate process $[x_1\ x_2]$, each lasting 1000 samples, were generated. Auto- and cross-spectral density functions were estimated by means of the parametric approach, with model order $p = 10$. To perform spectral estimations, the bivariate AR model described by (3) was identified by the least-squares method, and the model hypotheses (i.e., whiteness and uncorrelation of the prediction errors, even at zero lag) were checked for the selected model order (Baselli et al. 1997). The coherence and the transfer function were then estimated by the traditional non-causal approach and by the causal approach and averaged over the 100 realizations.

3.2 Real data

To characterize typical cardiovascular and cardiorespiratory transfer functions in physiological conditions, the proposed method was applied on ten healthy young subjects (four women, 24.7 ± 1.6 years old). Surface ECG (lead II), finger photopletismographic arterial blood pressure (Finapres, 2300; Ohmeda, Englewood, CO, USA) and respiratory activity (by differential pressure transducer)

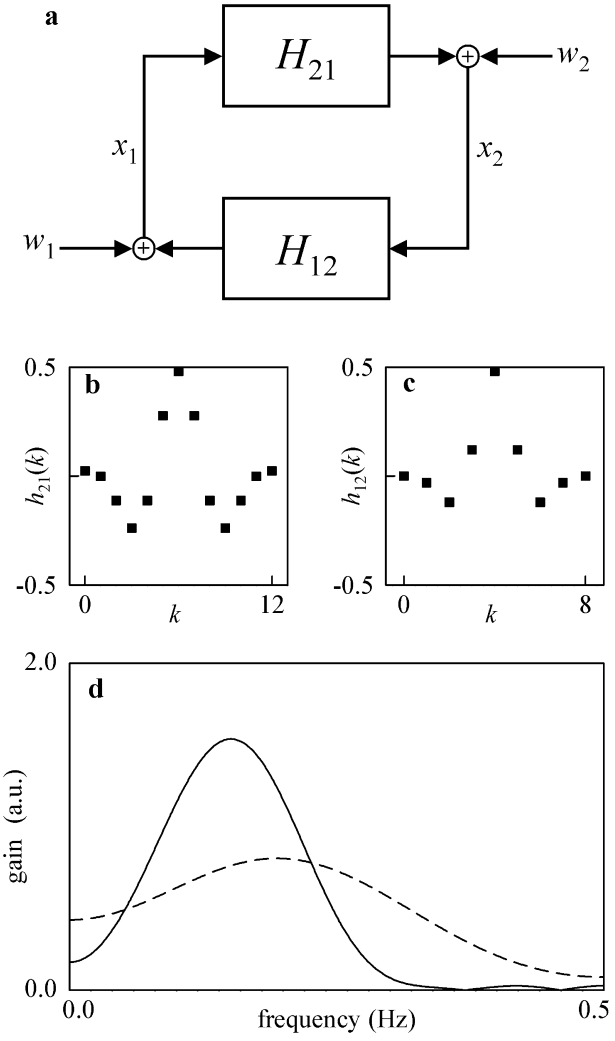

Fig. 2a–d. Closed loop bivariate process realized for the simulations. The simulated series x_1 and x_2 were obtained by the linear model depicted in **a**, starting from realizations of the gaussian white noise processes w_1 and w_2. The closed loop interactions between the two series were set by the linear transformations H_{21} and H_{12}, for which the time-domain coefficients are shown in **b** and **c** and the modulus of the frequency response is shown in **d** (*continuous line* for H_{21} and *dashed line* for H_{12})

were acquired in the morning in quiet ambience conditions, with subjects lying in a supine position and breathing spontaneously.

All signals were digitized with 1 KHz sampling rate and 12 bit resolution, and offline processed to beat-by-beat extract the variability series of heart period, systolic arterial pressure (SAP), and sampled respiration. At the i-th cardiac beat, the heart period $t(i)$ was measured from the ECG as the temporal interval between two consecutive R waves (RR interval), while the corresponding SAP and respiration values ($s(i)$ and $r(i)$) were obtained respectively by taking the local maximum of the arterial pressure signal inside the RR interval and by sampling the respiratory tracing in correspondence of the R-wave of the ECG at the onset of $t(i)$. With this measurement convention $s(i)$ is contained into $t(i)$, and thus a direct (not delayed) effect of RR interval on SAP is not possible. Moreover, with $r(i)$ taken at the onset of $t(i)$, immediate effects (within the same cardiac beat) from SAP or RR interval to respiration are unlikely. The length of the series selected for the analysis was set to 300 beats. As the acquired respiratory signal was not calibrated, the series r was normalized to allow the comparison among subjects. For each sampled respiration series, the normalization was performed sample-by-sample by subtracting the mean and by dividing by the standard deviation of the series.

In each subject, the transfer functions from respiration to SAP, from respiration to RR interval, and from SAP to RR interval were estimated by means of parametric cross-spectral analysis. To this end, the bivariate AR model described in (3) was identified for each pair of variability series. The identification procedure followed the least-squares method described in Baselli et al. (1997). The model order selection was performed by the Akaike criterion for multivariate processes (Akaike 1974), and the Anderson test (Kay 1988) was used to check for the whiteness and uncorrelation of the model residuals. The immediate effects were set according to the presented measurement conventions. After the identification procedure, coherence, gain and phase were estimated by the traditional non-causal approach and by the proposed causal approach. Furthermore, to assess whether the interaction between the two considered variables is unidirectional or bidirectional, the existence of a significant coupling in the direction opposite to that under analysis was tested by computing the corresponding causal coherence function as in Porta et al. (2002).

The two major rhythms usually studied in cardiovascular variability analysis are the one occurring at the frequency of the Mayer waves (low frequency (LF), from 0.04 to 0.15 Hz), and that triggered by respiration (high frequency (HF), ±0.04 Hz around the respiratory rate) (Pagani et al. 1986). Hence, in the presentation of the results we considered the values of coherence and transfer function sampled at LF and HF when the interactions between RR interval and SAP were modeled, and sampled at HF when the respiratory signal was involved. The statistical significance of the difference between non-causal and causal estimates of gain and phase evaluated in a given frequency band was assessed by means of the Student's t-test for paired data. A $p < 0.05$ was considered significant.

3.3 Testing the significance of the coupling

The significance of the coupling between two time series was assessed by means of a statistical test based on a surrogate data approach. One hundred pairs of surrogate series were obtained from the original by the AR fitting procedure (Faes et al. 2004). The original series were separately AR-fitted (Kay 1988), and the two obtained AR models were then fed with independent realizations of white noise to produce the surrogate pairs. The obtained surrogates preserved the autocorrelation but not the cross-correlation of the original series. The threshold for zero coherence was then obtained at each frequency as the 95th percentile of the distribution of the coherence estimated on the surrogate pairs. Finally, the link between the two original series

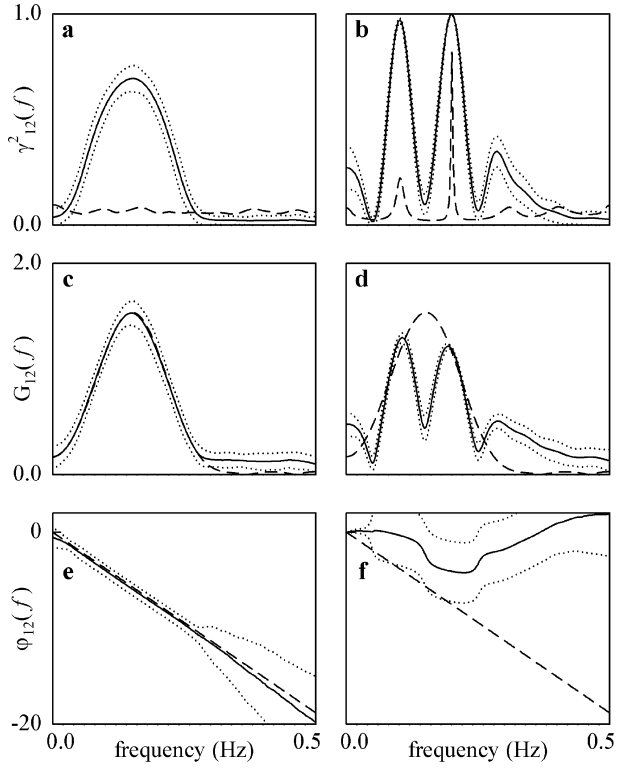

Fig. 3a–f. Coherence and transfer function estimated from the simulation model of Fig. 2 by the traditional non-causal approach. The estimates obtained in open loop condition ($H_{12} = 0$) and in closed loop condition ($H_{12} \neq 0$) are shown in **a**, **c**, **e** and in **b**, **d**, **f**, respectively. The coherence (**a**, **b**), gain (**c**, **d**) and phase (**e**, **f**) functions are plotted as mean (*continuous lines*) ± standard deviation (*dotted lines*) over 100 realizations of the simulation. The *dashed lines* represent the threshold for significance for the coherence (**a**, **b**), and the expected theoretical curves of gain (**c**, **d**) and phase (**e**, **f**)

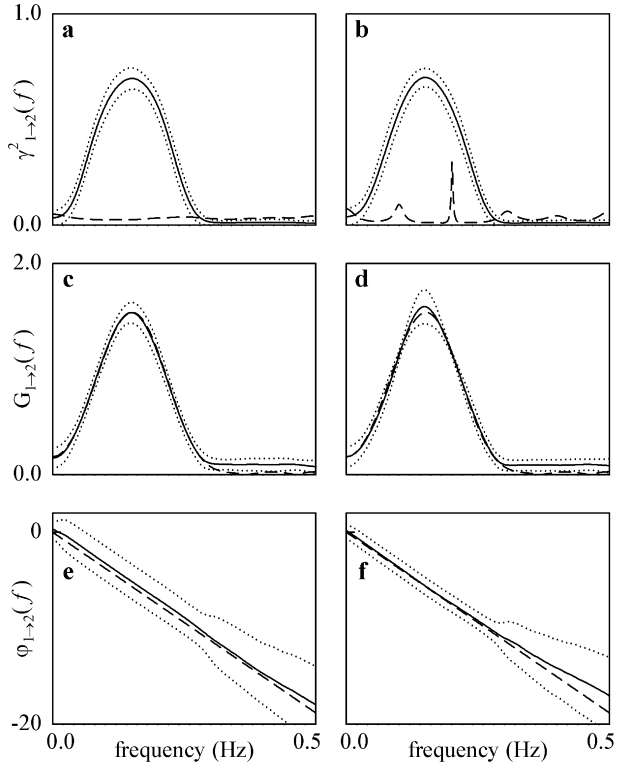

Fig. 4a–f. Coherence and transfer function estimated from the simulation model of Fig. 2 by the proposed causal approach. The estimates obtained in open loop condition ($H_{12} = 0$) and in closed loop condition ($H_{12} \neq 0$) are shown in **a**, **c**, **e** and in **b**, **d**, **f**, respectively. The causal coherence (**a**, **b**), gain (**c**, **d**) and phase (**e**, **f**) functions are plotted as mean (*continuous lines*) ± standard deviation (*dotted lines*) over 100 realizations of the simulation. The *dashed lines* represent the threshold for significance for the causal coherence (**a**, **b**), and the expected theoretical curves of gain (**c**, **d**) and phase (**e**, **f**)

was considered significant if the estimated coherence was higher than the threshold function. The proposed surrogate approach was used for both causal and non-causal coherence estimation procedures.

4 Results

4.1 Simulation results

Figure 3 reports the curves of coherence, gain, and phase estimated by the traditional non-causal approach for the two presented simulation schemes. When the open loop simulation was considered, both gain (Fig. 3c) and phase (Fig. 3e) were maintained with respect to their expected trends. On the contrary, in condition of closed loop interaction between the two simulated series the non-causal approach failed in reproducing the theoretical transfer function behavior. Indeed, the estimated coherence of Fig. 3b shows two distinct peaks with values significantly higher than the zero-level threshold, and the corresponding gain (Fig. 3d) and phase (Fig. 3f) functions strongly deviate from the expected curves.

The results of the application of the proposed causal approach to the same simulation schemes are illustrated in Fig. 4. As shown by the very similar shapes of coherence (Fig. 4a, b), gain (Fig. 4c, d), and phase (Fig. 4e, f) for the two simulations, the coupling from x_1 to x_2 was detected not only in open loop, but also in closed loop condition. Thus, the use of the causal approach allowed us to reproduce, though with a slightly lower fidelity, the expected transfer function curves even when a reverse relation was simulated in addition to the direct influence under investigation.

4.2 Experimental results

Figure 5 reports a representative example of the three distinct transfer function analyses performed on a healthy young subject in resting condition. The recorded beat-to-beat series of respiration, SAP, and RR interval are shown in Fig. 5a–c. The coherence functions between respiration and SAP (Fig. 5d) and between respiration and RR interval (Fig. 5e) show a well-resolved peak at the respiratory frequency (about 0.3 Hz in this case). At that frequency, also the causal coherences from respiration to SAP (Fig. 5g) and from respiration to RR

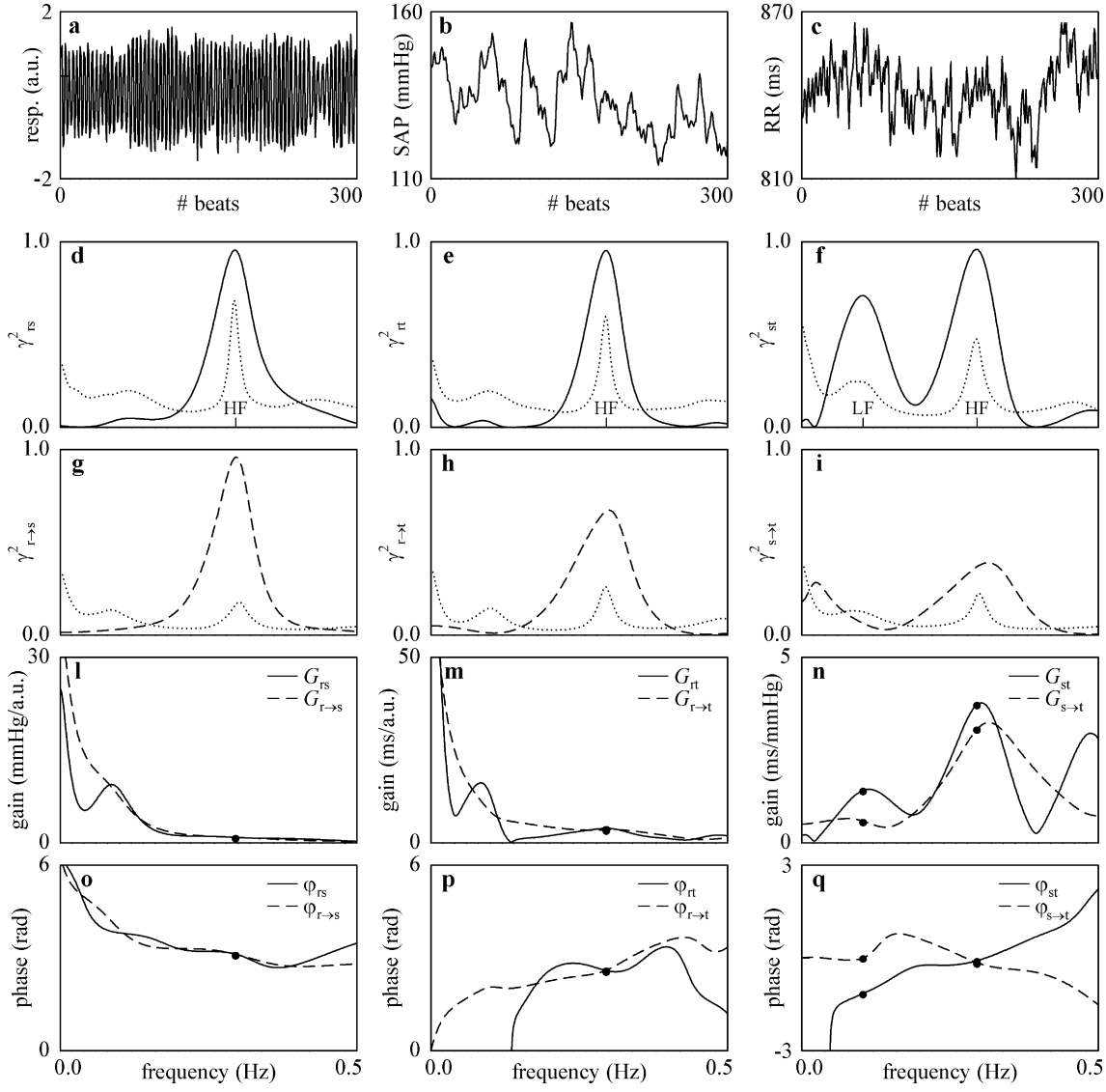

Fig. 5a–q. Estimation of coherence and transfer function by causal and non-causal approaches in a healthy man in supine position. The analyzed series of sampled normalized respiration, SAP, and RR are shown in **a**, **b**, and **c**. Coherence and transfer function are estimated from respiration to SAP (**d**, **g**, **l**, **o**), from respiration to RR (**e**, **h**, **m**, **p**), and from SAP to RR (**f**, **i**, **n**, **q**). The coherence (**d**, **e**, **f**, *continuous line*) and causal coherence (**g**, **h**, **i**, *dashed line*) are plotted together with their threshold for significance (*dotted lines*). The gain (**l**, **m**, **n**) and phase (**o**, **p**, **q**) functions are estimated by the non-causal method (*continuous lines*) and by the causal method (*dashed lines*). The *circles* indicate the values of gain and phase sampled at LF and HF

interval (Fig. 5h) are largely above the threshold for significance. The corresponding values of gain (Fig. 5l, m) and phase (Fig. 5o, p) estimated at HF by the traditional non-causal approach and by the proposed causal method are nearly the same. The coherence between systolic pressure and heart period is significant in both LF and HF bands (Fig. 5f). Differently, the causal coherence from SAP to RR interval (Fig. 5i) is above the threshold for significance only at HF, while it is not significant at LF. The corresponding causal and non-causal estimates of the transfer function (gain: Fig. 5n; phase: Fig. 5q) are quite different at LF, and similar at HF.

The values of traditional and causal transfer functions from respiration to SAP and from respiration to RR interval, sampled at HF for the ten analyzed subjects, are shown in Fig. 6 and Fig. 7, respectively. For both transfer function analyses, the distributions of gain (Figs. 6a and 7a) and phase (Figs. 6b and 7b) estimated by the causal and the non-causal approaches were not statistically different (p = NS). The values of coherence and causal coherence resulted above the threshold for significance for all subjects. Differently, the causal coherence functions estimated at HF on the reverse causal direction (i.e., with RR interval or SAP as input and respiration as output) were below the zero-level threshold in all subjects.

Results concerning the estimation of the transfer function from SAP to RR interval sampled at LF and HF are summarized in Fig. 8. The causal gain resulted significantly lower than the traditional one in both LF (Fig. 8a) and HF (Fig. 8c) bands. Similar results were obtained for

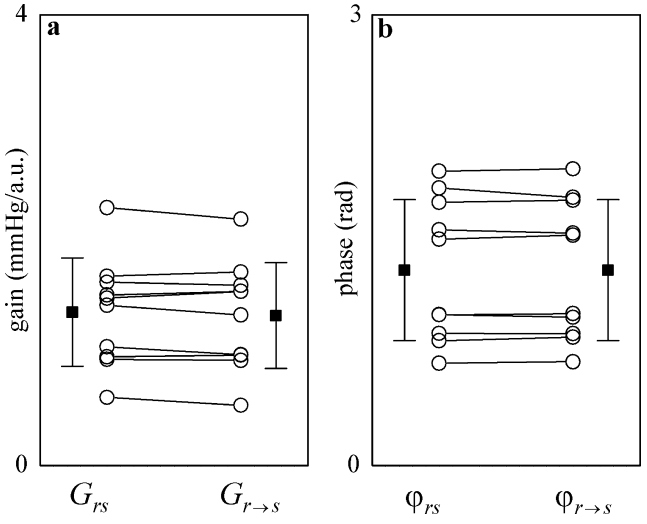

Fig. 6a, b. Values of the transfer function from respiration to SAP estimated in HF band for the ten analyzed subjects. The gain and phase obtained by the non-causal approach (G_{rs} and φ_{rs}) and by the causal approach ($G_{r\to s}$ and $\varphi_{r\to s}$) are shown in **a** and **b**, respectively

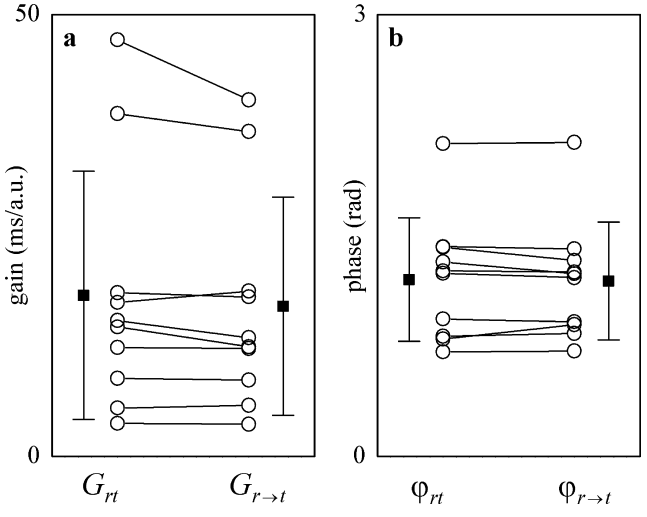

Fig. 7a, b. Values of the transfer function from respiration to RR estimated in HF band for the ten analyzed subjects. The gain and phase obtained by the non-causal approach (G_{rt} and φ_{rt}) and by the causal approach ($G_{r\to t}$ and $\varphi_{r\to t}$) are shown in **a** and **b**, respectively

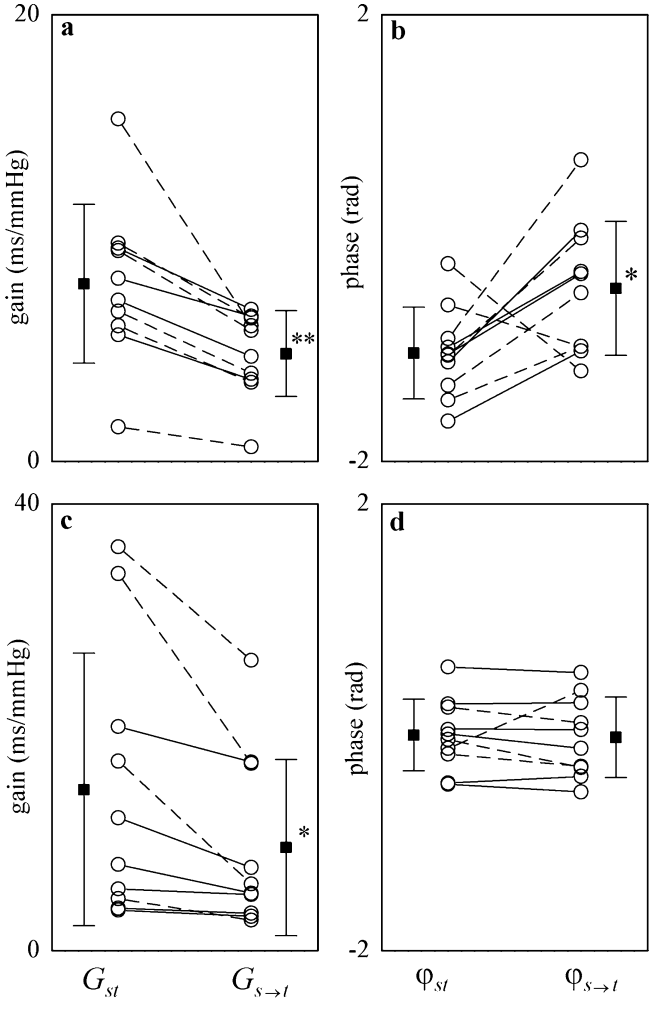

Fig. 8a–d. Values of the transfer function from SAP to RR estimated in LF band (**a**, **b**) and in HF band (**c**, **d**) for the ten analyzed subjects. The gain and phase obtained by the non-causal approach (G_{st} and φ_{st}) and by the causal approach ($G_{s\to t}$ and $\varphi_{s\to t}$) are shown in **a**, **c** and in **b**, **d**, respectively. *Dashed lines* correspond to subjects for which the causal coherence from SAP to RR was not significant. $^{*}p < 0.05$; $^{**}p < 0.01$, *t*-test for paired data

the LF phase, with significantly different values for the causal and non-causal approaches (Fig. 8b). Differently, the phase distributions estimated at HF were not statistically different (Fig. 8d). As regards the degree of coupling between RR interval and SAP, in all subjects the traditional coherence and at least one of the two causal coherences were above the threshold for significance in the two analyzed frequency bands. The causal coherence from SAP to RR interval was significant in four out of ten subjects at LF (continuous lines in Fig. 8a, b) and in six out of ten subjects at HF (continuous lines in Fig. 8c, d), while the causal coherence from RR interval to SAP was significant in nine out of ten subjects at LF and in six out of ten subjects at HF. A significant causal coherence in both directions (i.e., a closed loop interaction) was found in three subjects at LF and in two subjects at HF.

5 Discussion

The traditional method for estimating the linear transfer function between two time series is based on the estimation of their cross-spectral density function (Bendat and Piersol 1986). A major limitation of this approach is that the cross-spectral function cannot account for causality in the description of the link between the two series, while transfer function analysis assumes that the information between the two signals is exchanged on a specific causal direction. As a consequence, the resulting gain and phase estimates, that should describe the direct influence of the input over the output series, may be corrupted by the possible reverse effects. This limitation, clearly emerging from (1), (8) and (9), may lead to heavy misinterpretations

of the results deriving from transfer function analysis. In the present study, a causal approach for the evaluation of the linear transfer function between two time series was considered as an alternative to the traditional non-causal method. The proposed method makes use of the traditional definition of transfer function, and imposes causality, as suggested by Porta et al. (2002), by switching off the influences of the output series over the input one before the computation of the gain and phase functions. In this way, the transfer function may be correctly estimated even for closed loop interacting signals since the identification procedure is carried out in closed loop and by imposing causality.

The results of the proposed simulations confirmed that the traditional non-causal approach is not always appropriate for estimating the transfer function between two time series. Indeed, such method produced a reliable transfer function estimate when an open loop relationship from the input to the output series was set, while, in presence of a closed loop interaction, the estimated transfer function strongly deviated from the expected curves. This suggests that the traditional approach can be safely adopted only if reverse effects from the signal considered as output to that considered as input can be reasonably excluded. On the contrary, the causal transfer function was found to be reliable independently of the way by which the two investigated series are interacting, as the expected trends of gain and phase were well reproduced in both open and closed loop conditions.

As regards the application to real data, we found that at the frequency of HF oscillations the estimates of the causal transfer functions from respiration to SAP and to RR interval were not substantially different from those calculated by the traditional approach. This result may be interpreted by considering that in humans respiration interacts in an open loop way with arterial pressure, mainly through a mechanical mechanism (De Boer et al. 1987), and with heart rate, originating the well-known phenomenon of respiratory sinus arrhythmia (Hirsch and Bishop 1981). The existence of these open loop interactions was confirmed by the lack of linear coupling on the reverse path, as documented by the non-significant values found for the causal coherence from SAP or RR interval to respiration. Thus, the usual technique based on cross-spectrum calculation seems adequate to estimate the transfer function from respiration to other cardiac variables (Saul et al. 1989, 1991). On the contrary, the estimates of the transfer function from SAP to RR interval resulted significantly different when obtained by the causal and the non-causal approach, suggesting the absence of a pure open loop relationship between these two series. Indeed, in physiological conditions heart rate and arterial pressure are likely to affect each other as a consequence of the simultaneous feedback baroreflex regulation from SAP to RR interval and feedforward mechanical influence from RR interval to SAP (Koepchen 1984). In the present study, the importance of the contribution of the feedforward path is evidenced by the high number of subjects showing a significant casual coherence from RR interval to SAP. This result was observed even in an older population in Porta et al. (2002). Under those circumstances, the traditional transfer function analysis may produce unreliable results since the non-negligible reverse effects are incorporated into gain and phase estimates, while the causal transfer function should be more dependable as it is focused exclusively on the path from SAP to RR interval. These observations suggest that the modulus and the phase of the transfer function from SAP to RR interval derived from the traditional approach, usually taken as estimates of the baroreflex gain (Robbe et al. 1987) and of the latency on the baroreflex path (Cooke et al. 1999), are actually biased with an error depending on the strength of the coupling on the reverse causal direction (i.e., from RR interval to SAP). Particularly, we found that the gain function sampled in LF and HF bands is overestimated with respect to that obtained by the proposed causal method (see Fig. 8). This result agrees with recent studies developing specific open loop linear parametric models (Porta et al. 2000; Nollo et al. 2001) showing that gain estimates derived from the traditional bivariate model may be biased in presence of other regulatory mechanisms than the baroreflex. Even the phase function, when estimated via a non-causal approach, may be unreliable, especially when used to state which signal precedes the other (Taylor and Eckberg 1996).

Besides the analysis of the transfer functions, the calculation of traditional and causal coherence functions allowed us to investigate on the nature of the coupling between each pair of analyzed variables. The traditional coherence (Kay 1988) measures the strength of the coupling between the two variables accounting for both their reciprocal influences, while the causal coherence (Porta et al. 2002) focuses the coupling analysis on a specific causal verse. The traditional analysis was exploited to find out the existence of a significant coupling, and the causal approach was used to explore directionality in the coupling, thus allowing the detection of open or closed loop relationships. In addition, the accurate determination of the significance of the link between RR interval and SAP in a given frequency band, either on the traditional or on the causal coherence, was favored by the use of a frequency-dependent threshold for zero coherence (Porta et al. 2002; Faes et al. 2004). The traditional coherence resulted above the zero-level threshold for all the analyzed interactions and in all subjects, revealing the existence of a significant link between respiration, heart period and systolic pressure. In correspondence, the causal coherence displayed the dominant role played by respiration in originating the HF oscillations of SAP and RR interval, as documented by the detected open loop interactions, and revealed a more complicated pattern of cooperation between SAP and RR interval due to the presence of feedforward mechanical and feedback baroreflex paths sometimes simultaneously active. These results seem to suggest a reduced importance of the baroreflex contribution of SAP to RR interval with respect to the feedforward reverse influence of RR interval on SAP. Such circumstances should also limit the relevance of characterizing the transfer function from SAP to RR interval in healthy humans at rest, as the spontaneous variability of

the heart period could not be entirely related to baroreflex control mechanisms.

A basic assumption of the present and previous studies dealing with transfer function analysis is the existence of a linear relationship between the signals taken as input and output of the investigated system. It is worth noting that this prerequisite could be often violated in the application to cardiovascular and cardiorespiratory interrelations. For instance, some authors pointed out the presence of non-linear dynamics underlying the coupling between heart rate and arterial pressure (Nollo et al. 2002) or respiration (Hoyer et al. 1998). Hence, transfer function analysis should be applied only when the presence of a significant linear interaction between the investigated processes can be proven. Nevertheless, in specific conditions, such as small variations in the signals and analysis of the fluctuations in selected bands, the linearity assumption could be considered at least approximately valid. Several previous studies based on linear transfer function analysis have indeed adopted simple but useful models for the description of the interactions among cardiovascular and/or cardiorespiratory variables (de Boer et al. 1985; Robbe et al. 1987; Saul et al. 1991; Taylor and Eckberg 1996; Baselli et al. 1997; Wichterle et al. 2000; Porta et al. 2002). In this context, the growing body of literature about the expansion of linear models and the development of new non-linear algorithms opens new perspectives of comparison between these two different approaches. Particularly, the comparison between the linear causal analysis and the recently proposed methods of non-linear and phase synchronization (Palus 1997; Hoyer et al. 1998; Schafer et al. 1998; Porta et al. 1999) would be very useful to fully disclose the interrelations occurring in closed loop interacting processes.

In conclusion, the results of both simulations and application to real data suggest that the traditional non-causal approach to transfer function estimation is fully dependable only when the two analyzed series clearly interact in an open loop, while the presence of a significant link in the causal direction opposite to that under investigation may deviate gain and phase estimates from their true values. As a consequence, the proposed causal transfer function analysis is recommended whenever the open loop condition cannot be undoubtedly assessed, as is the case of the interactions between heart period and systolic pressure. Moreover, we suggest that in this type of interaction a reduced link from SAP to RR interval diminishes the relevance of the transfer function along the baroreflex path with respect to other mechanisms possibly regulating the variability of heart rate.

References

Akaike H (1974) A new look at the statistical model identification. IEEE Trans Autom Contr 19:716–723

Baselli G, Cerutti S, Civardi S, Liberati D, Lombardi F, Malliani A, Pagani M (1986) Spectral and cross-spectral analysis of heart rate and arterial blood pressure variability signals. Comput Biomed Res 19:520–534

Baselli G, Porta A, Rimoldi O, Pagani M, Cerutti S (1997) Spectral decomposition in multichannel recordings based on multivariate parametric identification. IEEE Trans Biomed Eng 44:1092–1101

Bendat JS, Piersol AG (1986) Random data. Wiley, New York

Cooke WH, Hoag JB, Crossman AA, Kuusela TA, Tahvanainen KUO, Eckberg DL (1999) Human response to upright tilt: a window on central autonomic integration. J Physiol 517: 617–628

de Boer RW, Karemaker JM, Strackee J (1985) Relationships between short-term blood-pressure fluctuations and heart-rate variability in resting subjects: a spectral analysis approach. Med Biol Eng Comput 23:352–358

de Boer RW, Karemaker JM, Strackee J (1987) Hemodynamic fluctuations and baroreflex sensitivity in humans: a beat-to-beat model. Am J Physiol 253:H680–H689

Faes L, Nollo G, Antolini R (2002) Experimental approach for testing the uncoupling between cardiovascular variability series. Med Biol Eng Comput 40:565–570

Faes L, Pinna GD, Porta A, Maestri R, Nollo G (2004) Surrogate data analysis for assessing the significance of the coherence function. IEEE Trans Biomed Eng 51:1156–1166

Hirsch JA, Bishop B (1981) Respiratory sinus arrhythmia in humans: how breathing pattern modulates heart rate. Am J Physiol 241:H620-H629

Hoyer D, Bauer R, Walter B, Zwiener U (1998) Estimation of nonlinear couplings on the basis of complexity and predictability — a new method applied to cardiorespiratory coordination. IEEE Trans Biomed Eng 45:545–552

Kay SM (1988) Modern spectral estimation. Theory and application. Prentice Hall, Englewood Cliffs

Koepchen HP (1984) History of studies and concepts of blood pressure waves. In: Miyakawa K, Polosa C, Koepchen HP (eds) Mechanisms of blood pressure waves. Springer, Berlin Heidelberg New York, pp 3–23

Legramante JM, Raimondi G, Massaro M, Iellamo F (2001) Positive and negative feedback mechanisms in the neural regulation of cardiovascular function in healthy and spinal cord-injured humans. Circulation 103:1250–1255

Nollo G, Porta A, Faes L, Del Greco M, Disertori M, Ravelli F (2001) Causal linear parametric model for baroreflex gain assessment in patients with recent myocardial infarction. Am J Physiol Heart Circ Physiol 280:H1830–H1839

Nollo G, Faes L, Porta A, Pellegrini B, Ravelli F, Del Greco M, Disertori M, Antolini R (2002) Evidence of unbalanced regulatory mechanism of heart rate and systolic pressure after acute myocardial infarction. Am J Physiol Heart Circ Physiol 283:H1200-H1207

Oppenheim AV, Schafer RW (1975) Digital signal processing. Prentice-Hall, Englewood Cliffs

Pagani M, Lombardi F, Guzzetti S, Rimoldi O, Furlan R, Pizzinelli P, Sandrone G, Malfatto G, Dell'Orto S, Piccaluga E, Turiel M, Baselli G, Cerutti S, Malliani A (1986) Power spectral analysis of heart rate and arterial pressure variabilities as a marker of sympatho-vagal interaction in man and conscious dog. Circ Res 59:178–193

Palus M (1997) Detecting phase synchronization in noisy systems. Phys Lett A 235:341–351

Pinna GD, Maestri R (2001) Reliability of transfer function estimates in cardiovascular variability analysis. Med Biol Eng Comput 39:338–347

Pinna GD, Maestri R, Raczak G, La Rovere MT (2002) Measuring baroreflex sensitivity from the gain function between arterial pressure and heart period. Clin Sci (Lond) 103:81–88

Pitzalis MV, Mastropasqua F, Massari F, Passantino A, Colombo R, Mannarini A, Forleo C, Rizzon P (1998) Effect of respiratory rate on the relationships between RR interval and systolic blood pressure fluctuations: a frequency-dependent phenomenon. Cardiovasc Res 38:332–339

Porta A, Baselli G, Lombardi F, Montano N, Malliani A, Cerutti S (1999) Conditional entropy approach for the evaluation of the coupling strength. Biol Cybern 81:119–129

Porta A, Baselli G, Rimoldi O, Malliani A, Pagani M (2000) Assessing baroreflex gain from spontaneous variability in conscious dogs: role of causality and respiration. Am J Physiol 279:H2558-H2567

Porta A, Furlan R, Rimoldi O, Pagani M, Malliani A, van de Borne P (2002) Quantifying the strength of the linear causal coupling in closed loop interacting cardiovascular variability signals. Biol Cybern 86:241–251

Priestley MB (1981) Spectral analysis and time series. Academic, London

Robbe HWJ, Mulder LJM, Ruddel H, Langewitz WA, Veldman JBP, Mulder G (1987) Assessment of baroreceptor reflex sensitivity by means of spectral analysis. Hypertension 10:538–543

Saul JP, Berger RD, Chen MH, Cohen RJ (1989) Transfer function analysis of autonomic regulation. II. Respiratory sinus arrhythmia. Am J Physiol 256:H153-H161

Saul JP, Berger RD, Albrecht P, Stein SP, Hui Chen M, Cohen RJ (1991) Transfer function analysis of the circulation: unique insights into cardiovascular regulation. Am J Physiol 261:H1231-H1245

Schafer C, Rosenblum MG, Kurths J, Abel HH (1998) Heartbeat synchronized with ventilation. Nature 392:239–240

Taylor JA, Eckberg DL (1996) Fundamental relations between short-term RR interval and arterial pressure oscillations in humans. Circulation 93:1527–1532

Wichterle D, Melenovsky V, Simek J, Necasova L, Kautzner J, Malik M (2000) Cross-spectral analysis of heart rate and blood pressure modulations. PACE 23:1425–1430